

Efficient Communication over Complex Dynamical Networks

Giacomo Baggio¹, Virginia Rutten^{2,3}, Guillaume Hennequin^{†4}, and Sandro Zampieri^{@†5}

¹Department of Mechanical Engineering, University of California, Riverside, California 92521, USA

²Gatsby Computational Neuroscience Unit, University College London, London W1T 4JG, UK

³Janelia Research Campus, Howard Hughes Medical Institute, Ashburn, VA, USA

⁴Computational and Biological Learning Lab, Department of Engineering, University of Cambridge, Cambridge CB2 1PZ, UK

⁵Dipartimento di Ingegneria dell'Informazione, Università degli Studi di Padova, via Gradenigo, 6/B I-35131 Padova, Italy

June 6, 2022

Abstract

In both natural and engineered systems, communication often occurs dynamically over networks ranging from highly structured grids to largely disordered graphs. To use, or comprehend the use of, networks as efficient communication media requires understanding of how they propagate and transform information in the face of noise. Here, we develop an information-theoretic framework that enables us to examine how network structure, noise, input coding, and interference between consecutive symbols jointly determine transmission performance in networks with linear dynamics at single nodes and arbitrary topologies. Mathematically normal networks, which can be decomposed into separate low-dimensional information channels, suffer greatly from readout noise. Interestingly, most details of their wiring have no impact on transmission quality. Non-normal networks, however, can largely cancel the effect of noise by transiently amplifying select input dimensions while ignoring others, resulting in higher net information throughput. Our theory could inform the design of new communication networks, as well as the optimal use of existing ones.

Reliable propagation of information through networks with unreliable nodes is a fundamental problem facing many engineered and natural systems. This includes social networks (Bakshy et al., 2012; Ver Steeg and Galstyan, 2012; Guille et al., 2013; Molaei et al., 2018; Bagrow et al., 2019), peer-to-peer networks (Decker and Wattenhofer, 2013), gene regulatory networks (Tkačik et al., 2008a,b; Tkačik and Walczak, 2011; Cheong et al., 2011; Selimkhanov et al., 2014), power grids (Hauser et al., 2005; Galli et al., 2011; Nardelli et al., 2014), and brain networks (Laughlin and Sejnowski, 2003; Akam and Kullmann, 2010; Mišić et al., 2014; Antonopoulos et al., 2015; Avena-Koenigsberger et al., 2018), to cite only a few. In order to engineer better communication networks, make better use of existing ones, or understand how natural (e.g. biological) networked systems function, a theory is needed that relates the network's connectivity and dynamics to its performance in transmitting information.

Previous work at the interface of network science and information theory has been largely restricted to static, feedforward networks, in which packets of activity travel one after the other through layers of memoryless nodes, with no interference. Examples include classic connectionist work where feedforward “neural” networks are optimized so their outputs retain as much information as possible about their inputs

(Oja, 1982; Hyvärinen and Oja, 1997; Toyozumi et al., 2005; Sharpee and Bialek, 2007; Toyozumi, 2012). These works have influenced how neuroscientists think about sensory pathways, which resemble layered networks of noisy neurons receiving input packets from body senses (Kandel et al., 2000). In particular, the neural representations of visual stimuli that are found along the primate ventral stream are strikingly similar to those that emerge in deep networks trained on object recognition tasks (Yamins and DiCarlo, 2016). More recent work (Shwartz-Ziv and Tishby, 2017) has drawn a link between deep learning (Goodfellow et al., 2016) and the information bottleneck method (Tishby et al., 2000), a principled approach to compressive communication. Beyond feedforward networks, the effect of recurrent topologies on information transmission was studied in the context of virtual electrical circuits (Rubido et al., 2017), but this was restricted to steady states and therefore disregarded any potential encoding of information in activity transients.

In most real-world scenarios, however, information does not propagate statically (or instantaneously), but dynamically within complex recurrent networks composed of non-memoryless nodes. The inherent dynamics of the network can greatly affect communication performance in ways that remain poorly understood. Kirst et al. proposed an analytical framework based atop standard notions of time-delayed mutual information and transfer entropy (Schreiber, 2000),

[@] To whom correspondence should be addressed: zampi@dei.unipd.it.

[†] Equal contributions.

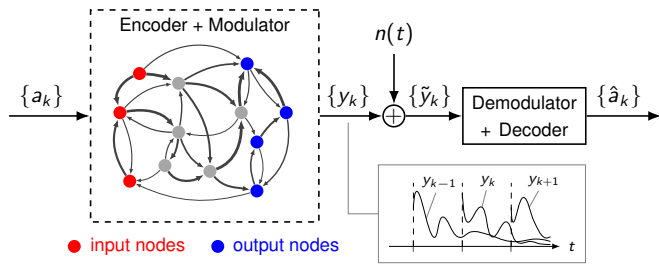


Figure 1 | Digital communication protocol. A sequence of discrete symbols $\{a_k\}$ is communicated by a sender to a receiver. Each symbol a_k is first encoded into a vector $u_k \in \mathbb{R}^m$ (“encoder”) which then excites the input nodes (red) of a complex network (Equation 1). The dynamics of this network act as a “modulator”, producing activation trajectories $y_k(t) = Ce^{A(t-kT)}Bu_k$ in some output nodes (blue). These are further corrupted by independent Gaussian noise $n(t)$ before reaching the receiver, where optimal decoding is used to retrieve the original symbol. Importantly, the modulator is not memoryless: due to first-order dynamics in each node of the network, patterns of network activity elicited by previously transmitted symbols linger and interfere with the current communication, thus contributing an intrinsic source of noise.

to quantify the routing of small activity fluctuations propagating on top of oscillatory reference dynamics. While their framework allowed them to identify a generic mechanism capable of generating flexible information-routing patterns in the network, it is based on a small-noise approximation and therefore cannot fully capture the impact of noise on network communication. Moreover, the authors did not systematically study the role of network topology. Harush and Barzel investigated the interplay between the network topology and its dynamics. They found that patterns of information are governed by universal laws that depend only on a few relevant parameters of the network dynamics. However, the analysis was carried out in a deterministic setting, and the proposed information transfer metric — which quantifies the sensitivity of a dynamical system to local perturbations — lacks an explicit information-theoretic interpretation. Ganguli et al. used Fisher information theory to quantify the short-term memory storage capacity of networks governed by linear dynamics. In investigating this memory problem, which is a form of network communication through time, the authors were led to study the interactions between single-node dynamics, connectivity, and input statistics, similar to the theory we develop here. However, the network received a one-dimensional input, and temporal correlations were neglected.

Here, we study the role of graph topology on the quality of information transmission in noisy networks with otherwise simple, linear single-node dynamics. We establish a novel framework for quantifying the maximum amount of information about high-dimensional inputs that can be transmitted reliably through such networks. We apply our framework to various network architectures, ranging from simple, structured networks amenable to analytical derivations, to more complex, disordered networks that we investigate numerically. Critically, all the networks we consider here have memory, from which interference arises between the network’s response to multiple symbols transmitted in close succession, and constitutes a source of internal noise. We show that when the amount of noise present in the information channel is large, anisotropic (mathematically “non-normal”, Trefethen and Embree, 2005) networks that embed directed feedforward pathways perform better than isotropic (“normal”) ones. Moreover, we find that such non-normal networks can even entirely overcome the effect of noise in some limit. Our results provide fundamental limits to the amount of information that a network can propagate, and how these limits depends on some key network properties. We discuss how these bounds

can be achieved by using specific encodings of input symbols, and how they can be pushed further by, e.g., setting the transmission time per symbol to an optimal value that depends on the maximal length of the anisotropic paths in the network. We expect our theory to contribute to understanding the behaviour of natural networked systems, which are often found to be strongly non-normal (Asllani et al., 2018). Further dissection of the mechanisms at work in natural networks (e.g. single-node dynamics, graph structure, adaptive wiring, ...) may also suggest better engineered solutions to network communication.

Results

Modelling framework

Communication through networks

We consider a standard digital communication protocol, whereby a sender transmits input symbols $\{a_k\}$ (taken from a finite alphabet), which are decoded by a receiver (Figure 1; see also Supplementary Note 1). Information transmission occurs via propagation of input symbols through a dynamic network. In order to obtain analytical, interpretable results that hold for arbitrarily complex graph topologies, we assume minimalistic dynamics for single network nodes: first-order, linear responses to inputs. Specifically, we consider continuous linear dynamical systems of the form

$$\begin{aligned} \frac{dx(t)}{dt} &= Ax(t) + B \sum_{k \geq 1} u_k \delta(t + kT), \\ y(t) &= Cx(t), \end{aligned} \quad (1)$$

where $x(t) \in \mathbb{R}^n$ denotes the state vector and $A \in \mathbb{R}^{n \times n}$ is the state matrix. We restrict our analysis to the case of “stable” network dynamics, whereby responses to transient inputs do not grow unbounded (which would be physically unfeasible) but fade away after some time. Mathematically, this means we require all eigenvalues of A to have negative real part.

Each symbol a_k in the sequence to be transmitted is first encoded as a vector $u_k \in \mathbb{R}^m$. Each of these inputs is then delivered as an impulse (here modelled as a Dirac’s delta $\delta(\cdot)$) that excites the network dynamics in Equation 1. Transmission of successive symbols occurs every T units of time. The

columns of the matrix $B \in \mathbb{R}^{n \times m}$ define “input nodes” (red circles in [Figure 1](#)), which are the only ones affected by the impulse. Likewise, a readout matrix $C \in \mathbb{R}^{p \times n}$ singles out specific output nodes (blue circles) whose activations $y_k(t)$ are transmitted to the receiver, further corrupted by independent Gaussian noise of variance σ^2 . The receiver is then assumed to perform optimal decoding (not explicitly modelled here) of these corrupted and overlapping output trajectories $\tilde{y}_k(t)$ to retrieve the sequence of transmitted symbols.

By reducing the complexity of single node dynamics to simple first-order evolution, [Equation 1](#) allows us to focus on the effect of network architecture (matrices A , B , and C) on the quality of information transmission. For example, [Equation 1](#) is known as a “rate equation” in computational neuroscience, whereby it has been shown to capture key aspects of the dynamics of neuronal networks around fixed points ([Dayan and Abbott, 2001](#); [Vogels et al., 2005](#)). Indeed, single neurons are often characterized by input/output functions that remain approximately linear over their relevant dynamic range ([Priebe and Ferster, 2008](#); [Inagaki et al., 2019](#)). In that case, A represents the matrix of synaptic connection weights, and $x(t)$ is interpreted as momentary deviations from steady-state firing rates.

Importantly, since each network node is governed by first-order dynamics, the network is not memoryless: activity trajectories elicited by previous communications interfere with (in fact, add linearly to) the network trajectory carrying information about the current input. Thus, for the transmission of a symbol at time $t = 0$ (assuming many symbols have already been transmitted), interference contributes an additional source of noise $i(t)$, given by

$$i(t) = \sum_{k=1}^{\infty} C e^{A(t+kT)} B u_{-k}. \quad (2)$$

This phenomenon, known as inter-symbol interference in communications ([Sklar, 2001](#)), arises in any communication medium that has some form of memory, including networks with node dynamics described by differential equations.

In the following, we study the combined effects of the network architecture (matrix A), communication time window (T), noise level (σ^2), and encoding of input symbols under this communication paradigm. We begin by establishing an analytical framework to characterize the quality of information transmission through the network, and highlight the trade-off that arises between sending symbols at a high temporal rate and the ability for the receiver to accurately decode them. We then summarize our analytical results, and illustrate them using appropriate network architectures.

Information transmission metrics

To quantify the amount of information that can be reliably propagated through the network channel described above, we use the well-known notion of channel capacity, first introduced by C. E. Shannon ([Shannon, 1948](#)). Due to the noisy nature of the channel, the transmission of an input symbol a , deterministically encoded into an input vector u , induces a

conditional probability distribution over corrupted trajectories of network output over the time window $[0, T]$, $p_T(\tilde{y}_{0:T}|u)$. The amount of information (in bits) about u contained in $\tilde{y}_{0:T}$ is measured by the mutual information

$$\mathcal{I}_T(u, \tilde{y}_{0:T}) = \int p(u) du \int p_T(\tilde{y}_{0:T}|u) \log_2 \frac{p(u)p_T(\tilde{y}_{0:T}|u)}{p(u)p_T(\tilde{y}_{0:T})} d\tilde{y}_{0:T}, \quad (3)$$

where the \cdot_T notation emphasises the dependence of mutual information on the transmission window, brought about by inter-symbol interference (a more formal definition of the integral over functions $\tilde{y}_{0:T}$ in [Equation 3](#) is given in Supplementary Note 3). To best utilise the channel, the sender must use the encoding distribution $p(u)$ that maximizes the mutual information; this optimum defines the channel capacity:

$$\mathcal{C}_T = \max_{p(u)} \mathcal{I}_T(u, \tilde{y}_{0:T}). \quad (4)$$

Shannon’s channel coding theorem guarantees that there exists an encoding scheme (and a matching decoding algorithm) mapping the discrete symbols $\{a_k\}$ onto inputs $\{u_k\}$ such that $2^{\mathcal{C}_T}$ different symbols can be reliably transmitted (i.e. with arbitrarily small decoding error probability) through the channel ([Cover and Thomas, 2012](#)). Although these capacity-achieving encoding/decoding algorithms can be very complex (cf. [Hochwald and Ten Brink \(2003\)](#)), \mathcal{C}_T provides a useful theoretical limit on communication throughput.

In [Equation 4](#), the maximization over the encoding distribution $p(u)$ must be performed with an additional constraint on the input power. Theoretically, this is required so that the capacity remains finite (the signal-to-noise ratio can be made arbitrarily large if inputs can be arbitrarily large too). In practice, the nodes of any physical network have limited dynamic range, and therefore network inputs must be power-limited. Here, the input distribution that achieves the capacity is a Gaussian distribution over input patterns with zero mean and covariance Σ , and the power constraint takes the form $\text{tr}(\Sigma) = 1$ (without loss of generality; cf. Supplementary Note 4).

An expression for the channel capacity

Our main theoretical result is the following expression for the channel capacity (Supplementary Note 3):

$$\mathcal{C}_T = \frac{1}{2} \max_{\Sigma \succcurlyeq 0, \text{tr} \Sigma = 1} \log_2 \frac{\det(\sigma^2 I + \mathcal{O} \mathcal{W})}{\det(\sigma^2 I + \mathcal{O}(\mathcal{W} - B \Sigma B^T))}, \quad (5)$$

where, in control-theoretic terms, \mathcal{O} denotes the observability Gramian over the interval $[0, T]$ of the system in [Equation 1](#), \mathcal{W} is the infinite-horizon controllability Gramian of the dynamics in [Equation 1](#) discretized with sampling time T and input matrix $B \Sigma^{1/2}$ ([Hespanha, 2009](#)). The formal definition and intuitive meaning of each of these matrices is discussed in our Supplementary Note 2. Note that [Equation 5](#) still involves a (difficult) maximization over the input distribution (via its covariance matrix Σ); in the following, we perform this optimization analytically where possible, but otherwise numerically using efficient algorithms ([Methods](#)).

The channel capacity affords a few intuitive properties (cf. Supplementary Note 4). First, \mathcal{C}_T always grows with increasing SNR $= 1/\sigma^2$. Second, \mathcal{C}_T is a bounded function of T that

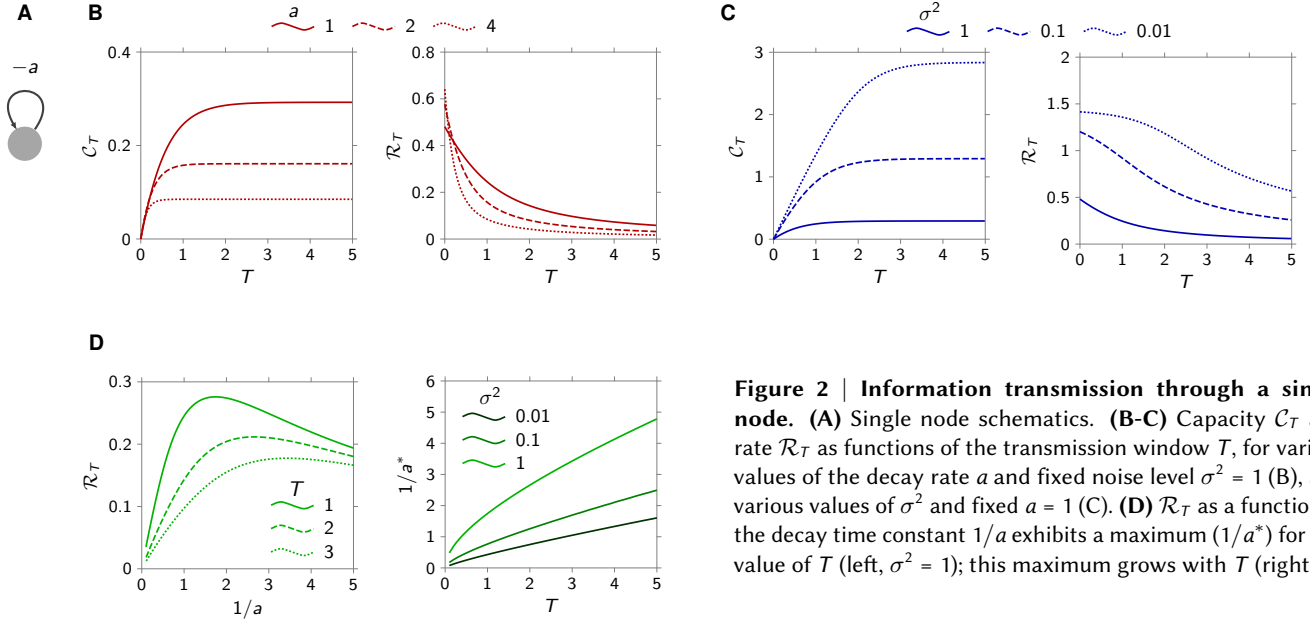


Figure 2 | Information transmission through a single node. (A) Single node schematics. (B-C) Capacity \mathcal{C}_T and rate \mathcal{R}_T as functions of the transmission window T , for various values of the decay rate a and fixed noise level $\sigma^2 = 1$ (B), and various values of σ^2 and fixed $a = 1$ (C). (D) \mathcal{R}_T as a function of the decay time constant $1/a$ exhibits a maximum ($1/a^*$) for any value of T (left, $\sigma^2 = 1$); this maximum grows with T (right).

attains its maximum as T grows to infinity. This is because, for increasing T , (i) network activations left over from previous transmissions have more time to decay away, leading to weaker interference, and (ii) longer stretches of signal are available for decoding, allowing for better estimation of the input signal via additional filtering/de-noising. Third, \mathcal{C}_T cannot decrease if nodes are added to either the set of input nodes, or the set of output nodes (Figure 1).

We also note that, in our framework, propagation of information through the network occurs over a finite time window T , and symbols can only be transmitted one at a time. Thus, a more relevant measure of channel performance is the number of bits that can be reliably transmitted *per unit time*, i.e. the information rate defined as

$$\mathcal{R}_T = \frac{1}{T} \mathcal{C}_T. \quad (6)$$

Since the channel capacity is bounded (due to output noise and inter-symbol interference), \mathcal{R}_T always decreases with T for large enough T . However, we will see that there often exists a non-zero optimal transmission window T , at which \mathcal{R}_T reaches a maximum.

The limitations of normal networks

As we will see later, many high-dimensional networks can be conveniently decomposed as a set of parallel, independent communication channels each transmitting information about a one-dimensional, scalar quantity. We therefore begin our analysis of the role of connectivity in network communication by an in-depth look at a simple case, that of a single isolated node (Figure 2A). With $B = C = \Sigma = 1$, and $A = -a < 0$ (where $1/a > 0$ is the node's decay time constant), Equation 5 simplifies considerably, yielding the following capacity:

$$\mathcal{C}_T = \frac{1}{2} \log_2 \frac{2a\sigma^2 + 1}{2a\sigma^2 + e^{-2aT}}. \quad (7)$$

This expression illuminates some additional properties of the channel capacity and its dependence on network parameters. To begin with, \mathcal{C}_T grows with the allotted transmission window T (Figure 2B and C, left). Intuitively, this is because increasing the transmission window reduces inter-symbol interference, as the node's activity has more time to decay away before the next symbol is transmitted. However, while \mathcal{C}_T grows linearly with T for small increasing T , it eventually saturates at a maximum value $\propto \log_2 \left(1 + \frac{1}{2a\sigma^2}\right)$ that grows both with the node's decay time constant ($1/a$; Figure 2B, left) and with the SNR ($1/\sigma^2$; Figure 2C, left). Indeed, for large enough T , the output noise becomes the main factor limiting the capacity, and grows increasingly dominant during the transmission of a symbol as the node's activity (the "signal") decays exponentially over time. Thus, increasing the observation time T cannot indefinitely increase the ability of an ideal observer to reconstruct the input symbol.

Next, as T increases with diminishing returns on the capacity (cf. above), the rate (information per unit time, Equation 6) is bound to decrease (Figure 2B and C, right). Thus, keeping the transmission window very short is the most effective way for a single node to transmit information under time pressure. In this limit, $\mathcal{R}_{\max} = \frac{1}{\ln 2} \frac{a}{1+2a\sigma^2}$ bits/s can be transmitted.

In practice though, transmission windows cannot be made arbitrarily small. For example, visual information conveyed to the brain via the optic nerve fluctuates on a timescale that is limited "at the source" by the rate at which objects move in the scene, and by the frequency and speed of saccadic eye movements which determine an effective sampling frequency. Thus, we now assume a finite transmission window $T > 0$. In this case, there exists an optimal value of the decay time constant $1/a$ for both \mathcal{R}_T (Figure 2D, left) and \mathcal{C}_T (not shown). This reflects a trade-off between the background noise and inter-symbol interference, mathematically evident from Equation 7, where \mathcal{C}_T can be seen to go to zero when a is either very small or very large. Intuitively, for small decay time constants $1/a$, inter-symbol interference becomes

irrelevant, and the channel capacity is limited by the effective signal to noise ratio $(1/a)/\sigma^2$, which in turn decreases with decreasing $1/a$. Similarly, for long decay times (increasing $1/a$), inter-symbol interference dominates, and ruins the channel capacity by letting the summed activities of many previous transmissions pollute the component relevant to the current symbol. Thus, the rate (and capacity) is expected to achieve a maximum for some intermediate, optimal value of the decay time constant. Numerically, we find that this optimal time constant scales near-linearly with the transmission window T (Figure 2D, right).

The case of a single-node “network” is, in fact, characteristic of the broader class of so-called “normal” networks, which include symmetric, skew-symmetric, and translation-invariant graphs to name only a few examples (mathematically, normality means $AA^\dagger = A^\dagger A$, where \cdot^\dagger denotes the conjugate transpose). Indeed, any normal network composed of n nodes can be shown to behave like a set of n independent scalar information channels (Supplementary Note 6), each corresponding to a specific spatial “mode” of activity at the network level that decays at a specific rate between consecutive transmission events. For example, for a translation-invariant architecture, these channels correspond to Fourier modes of varying spatial frequencies with decay rates that depend on the strength and spatial smoothness of the recurrent interactions (Ben-Yishai et al., 1995; Goldberg et al., 2004; Ganguli et al., 2008).

Our mathematical analysis of normal networks shows that, despite their appealing interpretation as sets of parallel communication sub-channels, these networks might not be optimally suited for transmitting information. First, as expected from an ensemble of independent scalar sub-channels whose rates \mathcal{R}_T each decrease with T (recall Figure 2B and C, right; further examples are given below), multidimensional normal networks too are best exploited in the limit of very small transmission windows ($T \rightarrow 0$). As discussed previously, this limit is irrelevant in most applications (where T is finite), implying that normal networks would always be sub-optimally exploited in practice. Second, and more importantly, we could show that the performance of a normal network does not depend on the fine details of its architecture (e.g. the detailed couplings between nodes) but only on the average decay rate of its nodes (the trace of A). Indeed, the information transmission rate of a normal network can never exceed (Supplementary Note 6)

$$\mathcal{R}_{\max} = \frac{1}{\ln 2} \frac{\text{tr}(A)}{2\sigma^2 \text{tr}(A) - 1}. \quad (8)$$

Critically, there are infinitely many network architectures that share the same $\text{tr}(A)$ but have otherwise very different geometries. It would be somewhat surprising if, among this very large set, the restricted subset of normal networks achieved the best performance. What is more, Equation 8 also implies that the maximum rate of any normal network in the low SNR regime is simply $\mathcal{R}_{\max} \approx \frac{1}{2 \ln 2 \sigma^2}$, which no longer depends on the connectivity matrix A . In other words, no amount of clever structuring of a normal architecture can ever rescue the drop in information rate incurred by a decrease in SNR. These considerations prompted us to study information transmission through more general, non-normal networks.

Role of non-normality in information transfer

A “non-normal” network is any network whose connectivity matrix A is not normal (Trefethen and Embree, 2005). Thus, given the equivalence of normal networks with independent parallel channels discussed above, a non-normal network is one that cannot be so decomposed. This implies the existence of effective feedforward pathways, embedded either explicitly at the level of network nodes (i.e. a tree-like structure that one would notice by looking at the connection graph) or implicitly at the level of orthogonal activity modes that involve many nodes simultaneously (“hidden” feedforward pathways; Goldman, 2009; Murphy and Miller, 2009; Hennequin et al., 2012). Mathematically, explicit and implicit tree-like structures can both be identified via the Schur decomposition $A = U\Delta U^\dagger$. If A is normal, this decomposition returns a diagonal matrix Δ , with the Schur modes (columns of U) interpreted as separate information channels with decay rates given by the diagonal of Δ . For a non-normal matrix A , the Schur decomposition returns a triangular Δ , the off-diagonal elements of which reveal hidden feedforward connections between the Schur modes.

While it is straightforward to classify a matrix as normal or non-normal, the extent to which a matrix departs from normality, and how such departure affects the dynamics of the network and communication performance, are more difficult to assess. To address this, we begin with a class of linear graphs whose departure from normality is parameterized by two characteristics that we can choose independently and arbitrarily: the length of the chains embedded in the graph, and the directionality of these chains (Figure 3A). The simplicity of this architecture allows us to conveniently decouple the effects of (i) the eigenvalues of A , and (ii) its departure from normality, on the network dynamics (see below). We show later that the insights obtained from this simple structured example topology, in particular concerning the role of network non-normality, carry over to higher-dimensional and heterogeneous networks.

Mathematically *normal* versions of this chain architecture are obtained either when there effectively is no chain (set of isolated nodes), or when there is no specific directionality in the connectivity ($\alpha = 1$, symmetric graph). In either case, the information rate decreases with increasing transmission window T (Figure 3B, lowest curves), consistent with the formal theory developed above. To understand this behaviour, and as a preliminary to our analysis of non-normal networks, we examine the optimal allocation of input power, or the spatial structure of the optimal input distribution. In Figure 3C, we plot the optimal input covariance Σ^* (calculated as part of deriving the capacity; recall Equation 5), expressed in the eigenbasis of the connectivity matrix A , with eigenvectors sorted by decreasing values of their decay rate. For long transmission windows, more of the input variance is funnelled through slow-decaying modes than through fast-decaying ones (right, $T \geq 0.5$). This allows more of the input signal to survive the natural decay of activity in the network, thereby sustaining the signal-to-noise ratio at the receiver. For shorter transmission windows, this strategy no longer pays off: much of what is “signal” for the current transmission is effectively “noise” for the next transmission epoch, and prolonging its

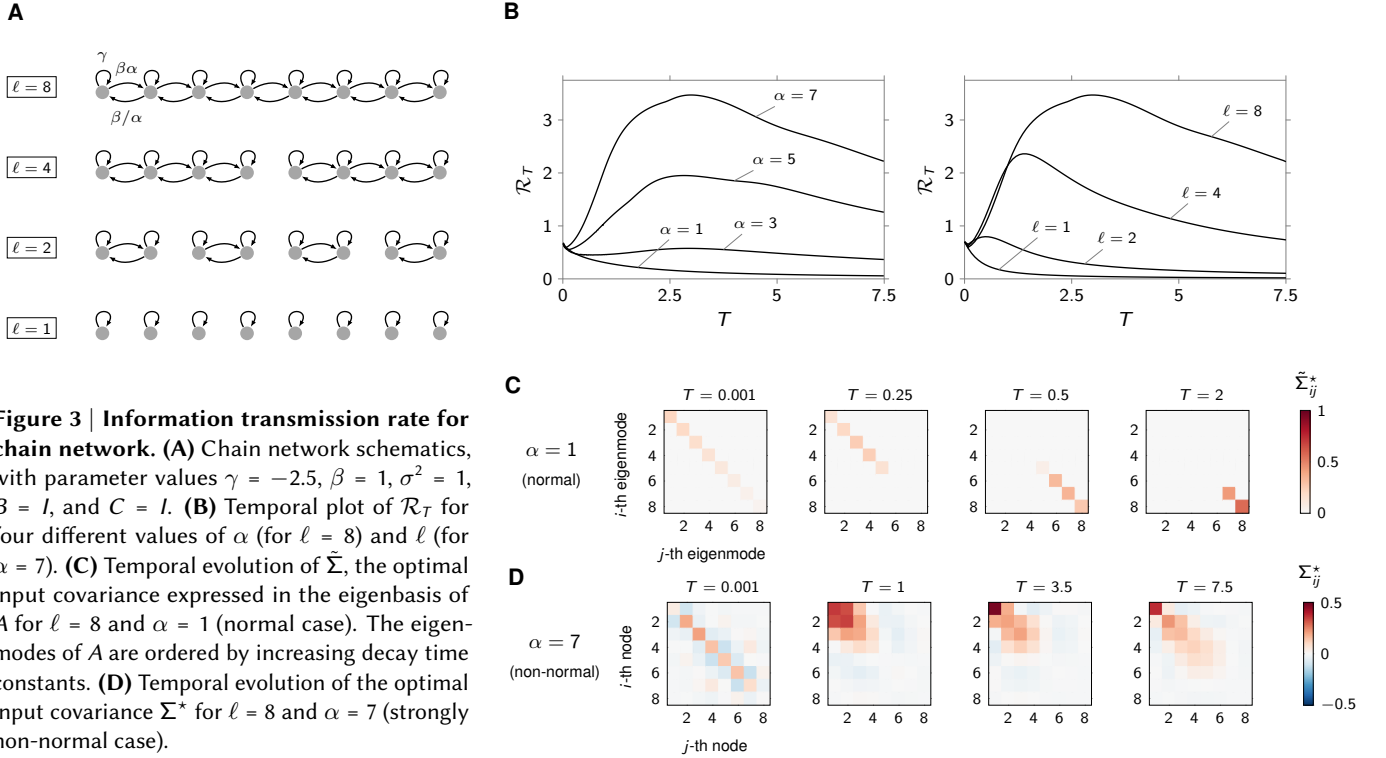


Figure 3 | Information transmission rate for chain network. (A) Chain network schematics, with parameter values $\gamma = -2.5$, $\beta = 1$, $\sigma^2 = 1$, $B = l$, and $C = l$. (B) Temporal plot of \mathcal{R}_T for four different values of α (for $l = 8$) and l (for $\alpha = 7$). (C) Temporal evolution of $\tilde{\Sigma}$, the optimal input covariance expressed in the eigenbasis of A for $l = 8$ and $\alpha = 1$ (normal case). The eigenmodes of A are ordered by increasing decay time constants. (D) Temporal evolution of the optimal input covariance Σ^* for $l = 8$ and $\alpha = 7$ (strongly non-normal case).

decay adds further inter-symbol interference. Accordingly, the optimal allocation strategy for short T is the opposite of that for large T : each sub-channel is now allocated power proportional to its decay rate (Supplementary Note 6). Finally, while achieving the channel capacity requires careful selection of sub-channels according to their decay rates (as just discussed), concentrating the input power on too few channels comes at a cost, as communication no longer exploits all the network’s degrees of freedom. This is best illustrated in a set of n independent nodes with identical time constants, for which the best strategy is provably to give each node an equal share P/n of the total available power (Supplementary Note 6). This amounts to maximizing the entropy of the input distribution. The covariances matrices of Figure 3C represent the optimal way of resolving the above trade-offs, for the chain architecture considered here.

We next show that large gains in information rate can be obtained by making the network connectivity non-normal. The degree of non-normality of the chain’s connectivity matrix ($l = 8$) can be increased, *without altering its eigenvalues*, by increasing a single parameter α reflecting the graph’s directionality (Figure 3A). As the network is made increasingly non-normal in this way, its information rate grows to eventually exceed the normal networks’ optimal rate by a large margin. Moreover, the optimal rate is now attained at some realistic, finite transmission window T (Figure 3B, left).

To understand the mechanism through which non-normality improves information transmission, we repeat our inspection of optimal power allocation, now for a non-normal network with $\alpha = 7$. In Figure 3D, we plot the optimal input covariances (no longer expressed in the eigenbasis of A , but in the standard basis of the network’s nodes) for various transmission window

lengths. For large transmission windows, including the one that leads to the largest rate \mathcal{R}_{\max} , input power concentrates on the “source” nodes (left-most nodes in Figure 3A, bottom). This optimal strategy exploits the network’s ability to amplify signals as they propagate down the chain towards the “sink” (the last node). Thus, the SNR at the receiver can display large transient increases, whereas its decay could at best be slowed down in normal networks. For short transmission windows, such a strategy no longer pays off, due to the same tradeoffs as uncovered above for normal networks. First, the signal transiently builds up into the next transmission epoch, where it no longer is signal but instead contributes noise. Second, distributing input power unevenly across the n network nodes by favouring the “source” nodes reduces the entropy of the input distribution, which fundamentally limits the information rate. Together, these drawbacks explain why the source nodes are not particularly favoured over sink nodes when T is small (Figure 3D, left), and why, in general, the input power does not concentrate entirely on the first node in the chain, but is generally distributed among the first few.

To further substantiate that non-normality benefits the channel capacity, we manipulate the degree of non-normality of the chain network discussed above, this time not by increasing α , but through a complementary modification. Specifically, we morph the non-normal chain discussed above back into a normal network, by chopping the original chain of length $l = 8$ into sets of shorter chains (Figure 3A, top to bottom). Shorter chains consistently yield smaller channel capacity (Figure 3B, right), confirming that network non-normality has a positive impact on information transmission.

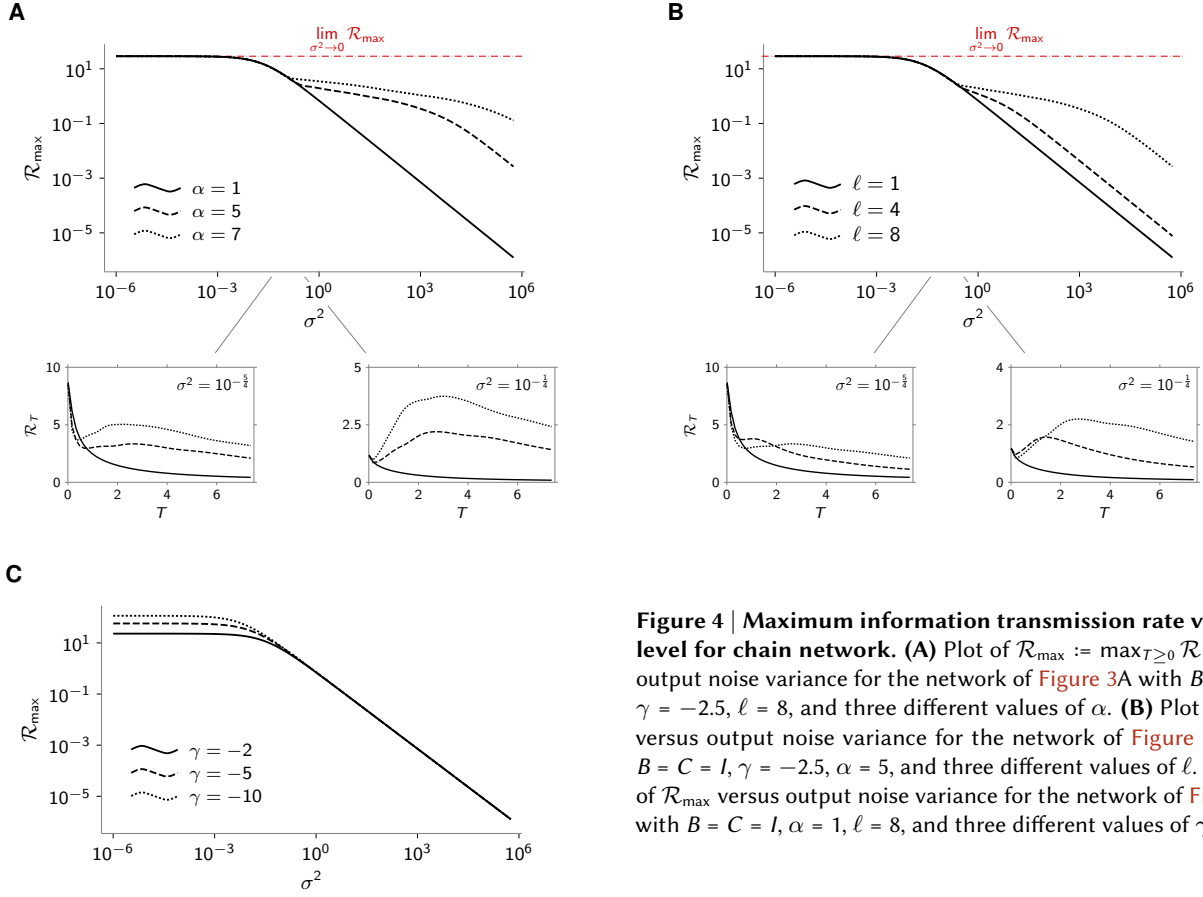


Figure 4 | Maximum information transmission rate vs. noise level for chain network. (A) Plot of $\mathcal{R}_{\max} := \max_{T \geq 0} \mathcal{R}_T$ versus output noise variance for the network of Figure 3A with $B = C = I$, $\gamma = -2.5$, $\ell = 8$, and three different values of α . (B) Plot of \mathcal{R}_{\max} versus output noise variance for the network of Figure 3A with $B = C = I$, $\gamma = -2.5$, $\alpha = 5$, and three different values of ℓ . (C) Plot of \mathcal{R}_{\max} versus output noise variance for the network of Figure 3A with $B = C = I$, $\alpha = 1$, $\ell = 8$, and three different values of γ .

How noise shapes the optimal architecture

The results presented so far show that non-normal architectures can, in principle, outperform normal networks as information transmission media. These results were obtained for fixed input SNR, and we now show that non-normality is all the more beneficial as the SNR is poor. To show this, we revisit the chain architecture of the previous section (Figure 3A) and systematically vary σ^2 , the amplitude of the noise at the receiver (Figure 4).

In the low-noise regime, non-normality has little impact on information transmission, whether the network is made non-normal by increasing its directionality (Figure 4A) or by increasing the length of its chains (Figure 4B). In fact, for small σ^2 , we have (cf. Supplementary Note 5)

$$\mathcal{R}_T \approx -\frac{1}{\ln 2} \text{tr}(A) = \frac{\gamma n}{\ln 2}, \quad (9)$$

which shows that the rate does not depend on the graph directionality α . For large enough σ^2 , however, increasing α or ℓ has pronounced benefits on the maximum information rate \mathcal{R}_{\max} (Figure 4A-B). In contrast, modifications of the parameters of the normal network ($\alpha = 1$) that affect the eigenvalues without causing any departure from normality have close to no impact on the transmission rate. Specifically, changing the decay rate γ of the single nodes is only beneficial in the low-noise regime (Figure 4C), corroborating the conclusions drawn from Equation 8 above. The same equation also predicts that changing the overall coupling strength β (while keeping

the directionality α constant) should have no effect on \mathcal{R}_{\max} (not shown).

From our analysis of this simple architecture, we conclude that network non-normality — i.e. the presence of effective directed pathways in the topology — can greatly enhance information transmission in the low SNR regime. In fact, we were able to show that non-normality can (in theory) cancel the effect of noise altogether (Supplementary Note 7). Specifically, no matter how poor the SNR is, it is always possible to increase the degree of non-normality of the network (by increasing α) and get arbitrarily close to the maximum transmission rate achievable in the *noiseless* regime (by any network with identical value of $\text{tr}(A)$; Figure 4A, horizontal dashed red line).

Intriguingly, this result does not only hold for the simple line architecture described above, but also for more complex class of networks with arbitrary “baseline topology” made increasingly non-normal through a process of “directed stratification” with a single free parameter α summarising departure from normality (Supplementary Note 7). In this family of models, as in the linear chain, the detrimental effect of output noise (however large) can be annihilated entirely by making the network sufficiently non-normal (by increasing α). In this limit of strong non-normality, the network effectively behaves as a one-dimensional, near-deterministic channel with decay rate given by $|\text{tr}(A)|$, and indeed achieves a transmission rate equal to that of any network with the same $\text{tr}(A)$ in the *absence of output noise* (Equation 9).

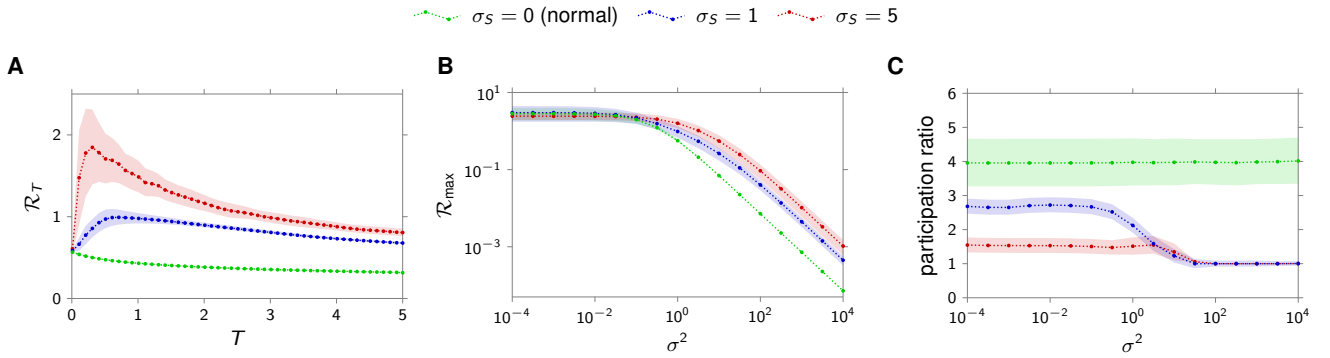


Figure 5 | Role of non-normality in high-dimensional, heterogeneous networks. (A) Rate as function of the transmission window T for $n = 20$, $\sigma^2 = 1$, $B = C = I$, and A drawn according to Equation 10. (B) Maximum rate $\mathcal{R}_{\max} := \max_{T \geq 0} \mathcal{R}_T$ as function of the readout noise variance σ^2 . (C) Effective dimensionality (quantified using the “participation ratio”, see Abbott et al., 2011 and Methods) of the input distribution that defines the optimal allocation of input power as function of the output noise variance σ^2 . In all panels, colors indicate the degree of non-normality (σ_S) of the network. Error bars denote 95% c.i. around the mean, estimated from 50 independent realizations of the 20×20 random matrix A , drawn according to Equation 10.

Generalization to heterogeneous topologies

Although the formulae we have derived regarding the information capacity of linear networks hold for arbitrary topology, most of the results presented so far were based either on highly simplified, small, and structured architectures (Figure 3A), or on networks that deviated from normality in a highly structured way (Supplementary Note 7). To assess the generality of our results, we now study larger and more heterogeneous networks whose departure from normality we can also control. Specifically, we generate random connectivity matrices A following Hennequin et al. (2014) as:

$$A = (-I + S)P. \quad (10)$$

Here P is a random positive definite matrix drawn from the inverse Wishart distribution (Methods), and S is a random skew-symmetric matrix whose (upper-triangular) elements are drawn independently from a normal distribution with zero mean and variance σ_S^2 . It is easily shown that any state matrix A drawn according to Equation 10 implies stable network dynamics, despite the network graph showing apparent disorder with connections of arbitrary average magnitude (e.g. there is no limit to the norm of P and S).

The degree of network non-normality is set by the parameter σ_S : when $\sigma_S = 0$, A is symmetric, hence normal; as σ_S increases, A departs further from normality. We calculated the maximum rate of such networks for various degrees of non-normality, and found a similar interplay between network non-normality, transmission window, and input SNR as in the simplified architecture of Figures 3 and 4. Specifically, non-normality results in greater maximum rates realized by non-zero optimal transmission windows (Figure 5A). Moreover, these benefits over normal networks only arise in the low SNR regime (Figure 5B). Finally, enhanced transmission performance at low SNR relies on a low-dimensional allocation of input power (Figure 5C).

The role of non-normality in information transmission is further illuminated by considering the limit of poor SNR

($\sigma^2 \rightarrow \infty$): for any transmission window length $T > 0$, the rate decays with growing σ^2 as (cf. Supplementary Note 5)

$$\mathcal{R}_T \approx \frac{1}{2 \ln 2 T} \frac{\|B^\top O B\|}{\sigma^2}, \quad (11)$$

where $\|B^\top O B\|$ represents the maximum total energy that the network can autonomously generate over a time window T , for an appropriate encoding of the input symbol u_0 . While the momentary magnitude of activity in normal networks can only decay in time (leading to sublinear growth of $\|B^\top O B\|$ with T , i.e. decreasing \mathcal{R}_T in Equation 11), non-normal networks have the capacity to transiently amplify certain input codes before the eventual decay of signals implied by collective stability. This leads to superlinear growth of $\|B^\top O B\|$ with T , which in turn results in transiently increasing \mathcal{R}_T peaking at some finite value of T (Equation 11).

Finally, in deriving Equation 11, we could also prove that in the limit of large input noise σ^2 , the information rate \mathcal{R}_T is realized by effectively one-dimensional inputs, whose distribution lies entirely along the most sensitive input direction (i.e. along the initial condition that evokes the largest energy in the window T ; Supplementary Note 5). In other words, the best way for the network to counteract a large amount of noise is to map every input symbol onto a single, maximally amplified input pattern, thus effectively giving up on most of its degrees of freedom. This corroborates and strengthens the generality of our findings of Figure 3D and Figure 5C regarding the effective dimensionality of the input distribution in the high-noise regime.

Discussion

In this paper we have proposed a novel framework to model information propagation through networks with arbitrary topology and nodes governed by linear dynamics. These dynamics imply a form of memory in single nodes, giving rise to interference between the activity transient initiated by the

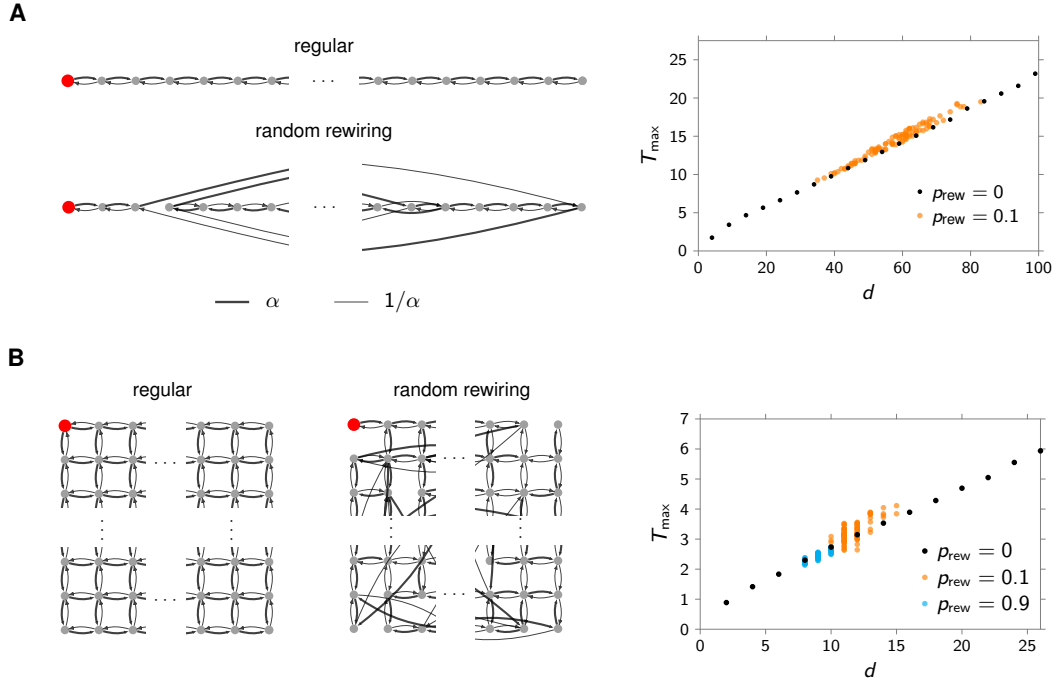


Figure 6 | Optimal transmission time vs. network diameter for “layered” non-normal chain and 2D lattice networks. (A) Plot of optimal transmission time T_{\max} against network diameter d (shortest path length between the two most distant nodes in the network) for a “layered” chain network with $\alpha = 5$, $\gamma = -2.5$ (self-loop weight, not shown), and $\sigma^2 = 10$. Top schematics and black dots: deterministic scenario wherein the chain dimension is varied from $n = 10$ to $n = 100$. Bottom schematics and orange dots: 100 realizations of a randomly rewired network of dimension $n = 100$ with rewiring probability $p_{\text{rew}} = 0.1$. **(B)** Plot of T_{\max} against network diameter d for a non-normal 2D lattice network with $\alpha = 5$, $\gamma = -2.5$ (self-loop weight, not shown), and $\sigma^2 = 10$. Left schematics and black dots: deterministic scenario wherein the 2D lattice dimension is varied from $n = 2^2$ to $n = 15^2$. Right schematics and colored dots: 100 realizations of a randomly rewired network of dimension $n = 15^2$ with two choice of rewiring probability $p_{\text{rew}} = 0.1, 0.9$. To reduce computational burden, in all plots the optimal input distribution is approximated by a rank one distribution. The latter distribution allocates all power to the red nodes in the figures and is found to yield a good approximation of the optimal input distribution at the maximum transmission rate, as shown in Figure 3D for the regular chain network. We refer to Methods for further details on the generation of the “layered” regular and random network topologies.

presentation of a given input symbol, and the activity left over from previous symbols. We have used the classic notions of Shannon channel capacity and rate to derive fundamental limits on communication performance, and studied how these limits depend on the network architecture. Our analysis has shown that the qualitative effects of graph connectivity on communication are largely determined by a property that is often overlooked: the degree of non-normality of the network’s (weighted) adjacency matrix. In particular, we have shown that normal networks perform poorly in the presence of large readout noise at the receiver. In contrast, non-normal networks exhibit more favorable communication properties, including the ability to entirely cancel out the effect of readout noise provided the input symbols are appropriately encoded, and the adjacency matrix is sufficiently non-normal. Interestingly, non-normal networks appear ubiquitous, with strong non-normality having been found in foodwebs, transport, biological, social, communication, and citation networks (Asllani et al., 2018).

Mechanistically, non-normal networks embed strongly feed-forward communication pathways (often buried in seemingly recurrent connectivity) along which input signals (preferentially delivered at the source) can progressively build up, yielding large gains that can overpower noise at the receiver. The

time it takes for signals to build up depends on the lengths of these feedforward pathways, and this is generally reflected in the existence of an optimal inter-symbol transmission time $T_{\max} := \arg \max_{T \geq 0} \mathcal{R}_T$. In fact, we found an interesting relationship between the optimal transmission time T_{\max} and a scalar summary statistics of the network’s connectivity: the so-called “network diameter” d (the shortest path length between the two most distant nodes in the network; Newman, 2018). We were able to empirically verify that $T_{\max} \propto d$, in several types of “layered” non-normal architectures (Figure 6 and Supplementary Note 7) with sufficiently strong output noise. For example, in a regular chain (Figure 6A, left), d scales with n , whereas in a regular 2D lattice (Figure 6B, left), it scales with \sqrt{n} — despite this qualitative difference, in both cases we found $T_{\max} \propto d$ (Figure 6A–B, right, black dots). Similarly, within each of these two classes, random rewiring (for a fixed n) causes substantial variations in diameter, which we found to cause coordinated variations in T_{\max} , again reflecting a linear relationship. Thus, a quick inspection of the network diameter may provide a cheap heuristic for setting the transmission time in practice, especially in high-dimensional scenarios where a direct numerical optimization of T using our theoretical bounds would be prohibitive.

Although our theory is limited to linear dynamics at each node,

we expect it to give useful approximations of the communication performance of weakly nonlinear networks that can be locally linearized. Even in more strongly nonlinear networks, Koopman operator-based approaches could yield good approximations of single nodes as linear, albeit higher-dimensional, systems (Williams et al., 2015; Mauroy and Gonçalves, 2016; Lusch et al., 2018), to which our theory would then directly apply. Nevertheless, we still expect nonlinearities to mitigate one of our main results concerning the limit of arbitrarily strong non-normality resulting in complete overcoming of output noise. For example, if neurons have a finite dynamic range (e.g. due to a saturation), the growth of signals propagating along feedforward pathways will remain limited, however long these pathways might be.

As is well known in the theory of non-normal operators (Trefethen and Embree, 2005), strong departure from normality often implies heightened sensitivity to structural perturbations — for example, the random addition/deletion of nodes or edges in a graph. This suggests a generic trade-off between communication performance and resilience, which would be interesting to study further. For example, we note that in the low-noise regime where normal networks can perform just as well as non-normal ones, constraints on robustness would favour normal networks. A similar trade-off has been identified recently in Pasqualetti et al. (2018) where network resilience was shown to be generically at odds with network controllability.

Our work may also offer new perspectives on memory and information storage. Information transmission and storage are very similar problems: communication is transmission through space, while memory is transmission through time. Indeed, these two problems admit very similar models, are often both approached using the tools of information theory (Ganguli et al., 2008; Toyozumi, 2012; Ganguli and Sompolinsky, 2010), and may interact in the context of network in ways that would be interesting to investigate further. Preliminary intuitions suggest that they may benefit each other: in our communication model, for example, inter-symbol interference could be entirely suppressed if one could keep a memory of decoded past symbols, and subtract their individual contributions to the momentary network activity at any time. Conversely, communication may improve memory. An obvious example is the oral tradition in human communities, where transmission of information from generation to generation emerges as a way to overcome the finite memory- (and indeed, life-) span of individuals.

Methods

Numerical computation of channel capacity and transmission rate. For vector-valued inputs ($m \geq 2$), the solution of the optimization problem in Equations 5 and 6 has been numerically carried out in Python using optimization routines from the Pymanopt library (Townsend et al., 2016), together with automatic differentiation techniques provided by Autograd (Maclaurin et al., 2015). If $B = C = I$ and A is normal, the solution is unique and admits a closed-form ex-

pression in terms of eigenvalues of A (Supplementary Note 6). More generally, if $C^\top C \succcurlyeq e^{A^\top T} C^\top C e^{AT}$, then the optimization in Equations 5 and 6 is convex (Supplementary Note 4), and so convergence to the maximum is always guaranteed using trust-region or steepest descent methods. Otherwise, the problem turns out to be, in general, non-convex, and, in order to avoid local maxima, we ran the latter routines several times (10^2 - 10^3), starting from different random initializations, and selected the largest outcome. Further, in the numerical evaluation of the capacity and transmission rate in Equations 5 and 6, the infinite-horizon discretized controllability Gramian

$$\mathcal{W} = \sum_{k=0}^{\infty} e^{AkT} B \Sigma B^\top e^{A^\top kT}$$

has been computed via the solution of the discrete-time algebraic Lyapunov equation

$$X - e^{AT} X e^{A^\top T} = B \Sigma B^\top,$$

whereas the observability Gramian over the interval $[0, T]$

$$\mathcal{O} = \int_0^T e^{A^\top t} C^\top C e^{At} dt$$

via numerical integration of the matrix-valued differential equation

$$\dot{X}(t) = A^\top X(t) + X(t)A + C^\top C,$$

subject to the initial condition $X(0) = 0$, cf. (Hespanha, 2009).

Generation of random non-normal matrices and participation ratio. In Equation 10, the skew-symmetric matrix $S \in \mathbb{R}^{n \times n}$ has been generated as $S = L - L^\top$, with $L_{ij} \sim \mathcal{N}(0, \sigma_S^2)$ for $i < j$, and $L_{ij} = 0$ otherwise. The positive definite matrix $P \in \mathbb{R}^{n \times n}$ has been drawn from the inverse Wishart distribution with scale matrix $\omega^{-2}I$ and ν degrees of freedom. We chose $\omega^{-2} = \nu - n - 1$, $\nu = 24 + n$, in order to guarantee sufficient heterogeneity in the eigenvalues of P (Hennequin et al., 2014). With this choice, it can be shown that σ_S^2 correlates well with standard measures of matrix non-normality. Following Abbott et al. (2011), given a positive definite matrix $A \in \mathbb{R}^{n \times n}$ with eigenvalues $\{\lambda_i\}_{i=1}^n$, we define the participation ratio

$$n_{\text{eff}} = \frac{(\sum_{i=1}^n \lambda_i)^2}{\sum_{i=1}^n \lambda_i^2}.$$

When applied to the covariance matrix, the participation ratio provides a measure of the effective dimensionality of the underlying random vector.

Computational details of Figure 6. The “layered” regular chain and 2D lattice networks in Figure 6 were generated as follows. First, we selected a node, say k , in the periphery¹ of a chain/2D lattice graph with unit weights (red node in the figures). Then, we applied to the network the “directed stratification” procedure described in Supplementary Note 7,

¹The periphery of a graph is the subset of nodes whose shortest path distance is equal to the diameter of the graph, cf. (Newman, 2018).

with input node k and directionality parameter $\alpha > 0$. To generate the “layered” random chain and 2D lattice networks, we applied the same procedure above to an i.i.d. randomly rewired (with probability p_{rew}) version of a bidirected chain/2D lattice graph with unit weights.

Code availability. The code used in this study is freely available in the public GitHub repository: http://github.com/baggiogi/commun_complex_networks.

References

- Abbott, L. F., Rajan, K., and Sompolinsky, H. (2011). Interactions between intrinsic and stimulus-evoked activity in recurrent neural networks. In Ding, M. and Glanzman, D., editors, *The Dynamic brain: an exploration of neuronal variability and its functional significance*, chapter 4, pages 65–82. Oxford University Press, Oxford.
- Akam, T. and Kullmann, D. M. (2010). [Oscillations and filtering networks support flexible routing of information](#). *Neuron*, 67(2):308–320.
- Antonopoulos, C. G., Srivastava, S., Pinto, S. E. d. S., and Baptista, M. S. (2015). [Do brain networks evolve by maximizing their information flow capacity?](#) *PLoS Comput. Biol.*, 11(8):e1004372.
- Asllani, M., Lambiotte, R., and Carletti, T. (2018). [Structure and dynamical behavior of non-normal networks](#). *Science advances*, 4(12):eaau9403.
- Avena-Koenigsberger, A., Misić, B., and Sporns, O. (2018). [Communication dynamics in complex brain networks](#). *Nat. Rev. Neurosci.*, 19(1):17.
- Bagrow, J. P., Liu, X., and Mitchell, L. (2019). [Information flow reveals prediction limits in online social activity](#). *Nat. Hum. Behav.*, 3:122–128.
- Bakshy, E., Rosenn, I., Marlow, C., and Adamic, L. (2012). [The role of social networks in information diffusion](#). In *Proceedings of the 21st international conference on World Wide Web*, pages 519–528.
- Ben-Yishai, R., Bar-Or, R. L., and Sompolinsky, H. (1995). [Theory of orientation tuning in visual cortex](#). *Proc. Natl. Acad. Sci. USA*, 92(9):3844–3848.
- Cheong, R., Rhee, A., Wang, C. J., Nemenman, I., and Levchenko, A. (2011). [Information transduction capacity of noisy biochemical signaling networks](#). *Science*, 334(6054):354–358.
- Cover, T. M. and Thomas, J. A. (2012). *Elements of information theory*. John Wiley & Sons.
- Dayan, P. and Abbott, L. F. (2001). *Theoretical neuroscience*, volume 806 of *Computational Neuroscience Series*. Cambridge, MA: MIT Press.
- Decker, C. and Wattenhofer, R. (2013). [Information propagation in the bitcoin network](#). In *Proceedings of the 2013 IEEE Thirteenth International Conference on Peer-to-Peer Computing (P2P)*, pages 1–10.
- Galli, S., Scaglione, A., and Wang, Z. (2011). [For the grid and through the grid: The role of power line communications in the smart grid](#). *Proc. IEEE*, 99(6):998–1027.
- Ganguli, S., Huh, D., and Sompolinsky, H. (2008). [Memory traces in dynamical systems](#). *Proc. Natl. Acad. Sci. USA*, 105(48):18970–18975.
- Ganguli, S. and Sompolinsky, H. (2010). [Short-term memory in neuronal networks through dynamical compressed sensing](#). In *Adv. Neural Inf. Process Syst.*, pages 667–675.
- Goldberg, J. A., Rokni, U., and Sompolinsky, H. (2004). [Patterns of ongoing activity and the functional architecture of the primary visual cortex](#). *Neuron*, 42:489–500.
- Goldman, M. S. (2009). [Memory without feedback in a neural network](#). *Neuron*, 61(4):621–634.
- Goodfellow, I., Bengio, Y., and Courville, A. (2016). *Deep learning*. MIT Press.
- Guille, A., Hacid, H., Favre, C., and Zighed, D. A. (2013). [Information diffusion in online social networks: A survey](#). *ACM Sigmod Rec.*, 42(2):17–28.
- Harush, U. and Barzel, B. (2017). [Dynamic patterns of information flow in complex networks](#). *Nat. Commun.*, 8:2181.
- Hauser, C. H., Bakken, D. E., and Bose, A. (2005). [A failure to communicate: next generation communication requirements, technologies, and architecture for the electric power grid](#). *IEEE Power Energy Mag.*, 3(2):47–55.
- Hennequin, G., Aitchison, L., and Lengyel, M. (2014). [Fast sampling-based inference in balanced neuronal networks](#). In *Adv. Neural Inf. Process Syst.*, pages 2240–2248.
- Hennequin, G., Vogels, T. P., and Gerstner, W. (2012). [Non-normal amplification in random balanced neuronal networks](#). *Phys. Rev. E*, 86(1):011909.
- Hespanha, J. P. (2009). *Linear systems theory*. Princeton university press.
- Hochwald, B. M. and Ten Brink, S. (2003). [Achieving near-capacity on a multiple-antenna channel](#). *IEEE Trans. Commun.*, 51(3):389–399.
- Hyvärinen, A. and Oja, E. (1997). [One-unit learning rules for independent component analysis](#). In *Adv. Neural Inf. Process Syst.*, pages 480–486.
- Inagaki, H. K., Fontolan, L., Romani, S., and Svoboda, K. (2019). [Discrete attractor dynamics underlies persistent activity in the frontal cortex](#). *Nature*, 566:212–217.
- Kandel, E. R., Schwartz, J. H., Jessell, T. M., Siegelbaum, S. A., and Hudspeth, A. J. (2000). *Principles of neural science*. McGraw-hill New York.
- Kirst, C., Timme, M., and Battaglia, D. (2016). [Dynamic information routing in complex networks](#). *Nat. Commun.*, 7:11061.

- Laughlin, S. B. and Sejnowski, T. J. (2003). [Communication in neuronal networks](#). *Science*, 301(5641):1870–1874.
- Lusch, B., Kutz, J. N., and Brunton, S. L. (2018). [Deep learning for universal linear embeddings of nonlinear dynamics](#). *Nat. Commun.*, 9:4950.
- Maclaurin, D., Duvenaud, D., and Adams, R. P. (2015). [Auto-grad: Effortless gradients in Numpy](#). In *ICML 2015 AutoML Workshop*.
- Mauroy, A. and Gonçalves, J. (2016). [Linear identification of nonlinear systems: A lifting technique based on the Koopman operator](#). In *Proceedings of the IEEE 55th Conference on Decision and Control (CDC)*, pages 6500–6505.
- Mišić, B., Sporns, O., and McIntosh, A. R. (2014). [Communication efficiency and congestion of signal traffic in large-scale brain networks](#). *PLoS Comput. Biol.*, 10(1):e1003427.
- Molaei, S., Babaei, S., Salehi, M., and Jalili, M. (2018). [Information spread and topic diffusion in heterogeneous information networks](#). *Sci. Rep.*, 8:9549.
- Murphy, B. K. and Miller, K. D. (2009). [Balanced amplification: A new mechanism of selective amplification of neural activity patterns](#). *Neuron*, 61(4):635–648.
- Nardelli, P. H. J., Rubido, N., Wang, C., Baptista, M. S., Pomalaza-Raez, C., Cardieri, P., and Latva-aho, M. (2014). [Models for the modern power grid](#). *Eur. Phys. J. Spec. Top.*, 223(12):2423–2437.
- Newman, M. (2018). *Networks*. Oxford university press, 2nd edition.
- Oja, E. (1982). [Simplified neuron model as a principal component analyzer](#). *J. Math. Biol.*, 15(3):267–273.
- Pasqualetti, F., Favaretto, C., Zhao, S., and Zampieri, S. (2018). [Fragility and controllability tradeoff in complex networks](#). In *2018 Annual American Control Conference (ACC)*, pages 216–221.
- Priebe, N. J. and Ferster, D. (2008). [Inhibition, spike threshold, and stimulus selectivity in primary visual cortex](#). *Neuron*, 57(4):482–497.
- Rubido, N., Grebogi, C., and Baptista, M. S. (2017). [Understanding information transmission in complex networks](#). *arXiv preprint, arXiv:1705.05287*.
- Schreiber, T. (2000). [Measuring information transfer](#). *Phys. Rev. Lett.*, 85(2):461.
- Selimkhanov, J., Taylor, B., Yao, J., Pilko, A., Albeck, J., Hoffmann, A., Tsimring, L., and Wollman, R. (2014). [Accurate information transmission through dynamic biochemical signaling networks](#). *Science*, 346(6215):1370–1373.
- Shannon, C. E. (1948). [A mathematical theory of communication](#). *Bell Syst. Tech. J.*, 27:379–423, 623–656.
- Sharpee, T. and Bialek, W. (2007). [Neural decision boundaries for maximal information transmission](#). *PLoS One*, 2(7):646.
- Shwartz-Ziv, R. and Tishby, N. (2017). [Opening the black box of deep neural networks via information](#). *arXiv preprint arXiv:1703.00810*.
- Sklar, B. (2001). *Digital communications: Fundamentals and applications*. Prentice Hall Upper Saddle River, 2nd edition.
- Tishby, N., Pereira, F. C., and Bialek, W. (2000). [The information bottleneck method](#). *arXiv preprint, arXiv:physics/0004057*.
- Tkačik, G., Callan, C. G., and Bialek, W. (2008a). [Information flow and optimization in transcriptional regulation](#). *Proc. Natl. Acad. Sci. USA*, 105(34):12265–12270.
- Tkačik, G., Callan Jr, C. G., and Bialek, W. (2008b). [Information capacity of genetic regulatory elements](#). *Phys. Rev. E*, 78(1):011910.
- Tkačik, G. and Walczak, A. M. (2011). [Information transmission in genetic regulatory networks: A review](#). *J. Phys. Condens. Matter*, 23(15):153102.
- Townsend, J., Koep, N., and Weichwald, S. (2016). [Pymanopt: A python toolbox for optimization on manifolds using automatic differentiation](#). *J. Mach. Learn. Res.*, 17(137):1–5.
- Toyoizumi, T. (2012). [Nearly extensive sequential memory lifetime achieved by coupled nonlinear neurons](#). *Neural Comput.*, 24(10):2678–2699.
- Toyoizumi, T., Pfister, J.-P., Aihara, K., and Gerstner, W. (2005). [Generalized Bienenstock–Cooper–Munro rule for spiking neurons that maximizes information transmission](#). *Proc. Natl. Acad. Sci. USA*, 102(14):5239–5244.
- Trefethen, L. N. and Embree, M. (2005). *Spectra and pseudospectra: The behavior of nonnormal matrices and operators*. Princeton University Press.
- Ver Steeg, G. and Galstyan, A. (2012). [Information transfer in social media](#). In *Proceedings of the 21st international conference on World Wide Web*, pages 509–518.
- Vogels, T. P., Rajan, K., and Abbott, L. F. (2005). [Neural network dynamics](#). *Annu. Rev. Neurosci.*, 28:357–376.
- Williams, M. O., Kevrekidis, I. G., and Rowley, C. W. (2015). [A data-driven approximation of the Koopman operator: Extending dynamic mode decomposition](#). *J. Nonlinear. Sci.*, 25(6):1307–1346.
- Yamins, D. L. K. and DiCarlo, J. J. (2016). [Using goal-driven deep learning models to understand sensory cortex](#). *Nat. Neurosci.*, 19(3):356.

Acknowledgements This work was supported by a Wellcome Trust Seed Award 202111/Z/16/Z (G.H.) and the Howard Hughes Medical Institute through a Janelia Graduate Research Fellowship (V.R.).

Author contributions G.B., V.R., G.H. and S.Z. all contributed to the conceptual and theoretical aspects of the study, and wrote the manuscript. G.B. carried out the numerical simulations and made the figures. G.B. and S.Z. wrote the supplementary material.

Competing financial interests The authors declare no competing interests.